Skeletal Radiology (2019) 48:285–292
https://doi.org/10.1007/s00256-018-2946-0

TECHNICAL REPORT

Differentiation between malignant and benign musculoskeletal tumors using diffusion kurtosis imaging

Masaki Ogawa[1] · Hirohito Kan[2] · Nobuyuki Arai[2] · Taro Murai[1] · Yoshihiko Manabe[1] · Yusuke Sawada[1] · Yuta Shibamoto[1]

Received: 27 November 2017 / Revised: 20 March 2018 / Accepted: 3 April 2018 / Published online: 9May 2018

Abstract

Objective The purpose of this study was to evaluate differences in parameters of diffusion kurtosis imaging (DKI) and minimum apparent diffusion coefficient (ADC_{min}) between benign and malignant musculoskeletal tumors.

Materials and methods In this prospective study, 43 patients were scanned using a DKI protocol on a 3-T MR scanner. Eligibility criteria were: non-fatty, non-cystic soft tissue or osteolytic tumors; > 2 cm; location in the retroperitoneum, pelvis, leg, or neck; and no prior treatment. They were clinically or histologically diagnosed as benign ($n = 27$) or malignant ($n = 16$). In the DKI protocol, diffusion-weighted imaging was performed using four b values (0-2000 s/mm^2) and 21 diffusion directions. Mean kurtosis (MK) values were calculated on the MR console. A recently developed software application enabling reliable calculation was used for DKI analysis.

Results MK showed a strong correction with ADC_{min} (Spearman's rs = 0.95). Both MK and ADC_{min} values differed between benign and malignant tumors ($p < 0.01$). For benign and malignant tumors, the mean MK values (± SD) were 0.49 ± 0.17 and 1.14 ± 0.30, respectively, and ADC_{min} values were 1.54 ± 0.47 and 0.49 ± 0.17 × 10^{-3} mm^2/s, respectively. At cutoffs of MK = 0.81 and $ADC_{min} = 0.77 \times 10^{-3}$ mm^2/s, the specificity and sensitivity for diagnosis of malignant tumors were 96.3 and 93.8% for MK and 96.3 and 93.8% for ADC_{min}, respectively. The areas under the curve were 0.97 and 0.99 for MK and ADC_{min}, respectively ($p = 0.31$).

Conclusions MK and ADC_{min} showed high diagnostic accuracy and strong correlation, reflecting the accuracy of MK. However, no clear added value of DKI could be demonstrated in differentiating musculoskeletal tumors.

Keywords Diffusion kurtosis imaging · Diffusion weighted imaging · Musculoskeletal tumor · MR imaging · Differentiation

Introduction

Magnetic resonance (MR) imaging is frequently used to characterize and stage musculoskeletal tumors. Diffusion-weighted imaging (DWI) is a non-contrast imaging technique that provides essential information on tumor composition, such as perfusion and cellularity, distinguishing between malignant and benign musculoskeletal tumors [1–4]. Many studies have reported that apparent diffusion coefficient (ADC) values in malignant musculoskeletal tumors are lower than in benign tumors [1–5]. However, the utility of ADC analysis is limited and previous studies reported a considerable overlap in the range of ADC values between benign and malignant tumors or no difference in ADC values [1–3].

Recently, the utility of diffusion kurtosis imaging (DKI), an advanced non-Gaussian diffusion imaging technique, was reported. Conventional DWI techniques always assume a Gaussian diffusion in which water molecules diffuse without any restriction. However, the water diffusion in complex biological tissues has a non-Gaussian distribution of water displacement profile in the presence of diverse barriers and compartmentalization that restrict the free displacement of water molecules. DKI calculates the kurtosis coefficient that signifies the deviation of tissue diffusion from a Gaussian model, which may be proportional to the heterogeneity and

✉ Masaki Ogawa
eternal@fj9.so–net.ne.jp

[1] Department of Radiology, Nagoya City University Graduate School of Medical Sciences, 1 Kawasumi, Mizuho-cho, Mizuho-ku, Nagoya 467-8601, Japan

[2] Department of Radiology, Nagoya City University Hospital, Nagoya, Japan

complexity of the microstructure and more suitable for assessment of the tumor microenvironment [6–11]. Previous studies showed that DKI parameters were more strongly correlated with the brain glioma grade and cellular proliferation compared to conventional ADC analysis [6, 7]. Also, several studies reported the utility of characterizing brain, head and neck, rectal, prostate, and breast tumors and assessing their response to therapy [8–11]. To the best of our knowledge, however, there have been no DKI studies on musculoskeletal tumors.

A problem in DKI is that the reliability may be insufficient, especially for non-brain imaging. DKI parameters are sensitive to noise effects and degradation of image quality, which strongly influence non-brain imaging [12, 13]. Also, there have been no specific products or software applications to analyze DKI, so the methods of analysis and calculation have been dependent on the user. However, a commercial DKI analysis software program has recently been developed in which the scan parameters and algorithm are optimized [14, 15]. We used this software on a 3-T MR scanner for reliable calculation in musculoskeletal tumors. The purpose of this study was to evaluate the differences in mean kurtosis (MK: a parameter of DKI) and ADC between malignant and benign non-fatty musculoskeletal tumors.

Materials and methods

Study design and patients

This prospective study was approved by the Institutional Review Boards of our hospital and registered on the University Hospital Medical Information Network Clinical Trial Registration (UMIN-CTR), Japan (registration number: UMIN000024381). Informed consent was obtained from patients before the examination and the privacy of the patients was completely protected. Eligibility criteria for entry were: (1) adult patients suspected of having or followed for a musculoskeletal tumor; (2) patient agreement to cooperate; (3) examination with the DKI sequence on the Hitachi 3-T MR scanner (Trillium Oval, Hitachi, Tokyo, Japan); (4) non-fatty, non-cystic soft tissue or osteolytic bone tumors; (5) tumor size larger than 2 cm; (6) tumor location in the retroperitoneum, pelvis, leg, or neck; and (7) no prior invasive treatment, radiation, or biopsy. The exclusion criteria were: (1) contraindications to MR (incompatible metal implants or pacemakers); (2) diagnostically unacceptable artifacts (motion or susceptibility artifacts, for example) on the images; and (3) proof of no tumor, inflammatory lesion, malignant lesion sustaining remission, or uncertain diagnosis. We evaluated fatty and cystic changes by using T2-weighted images and fat-saturated T2-weighted images on MR or CT images. We defined osteolytic bone tumor as that showing soft tissue density (approximately 20–80 Hounsfield units), not including calcification on CT images. We limited the tumor size to > 2 cm to avoid partial volume effects because the scan slice thickness was 5 mm. We did not include chest, abdominal, or hand tumors because susceptibility or motion artifacts caused by air or breathing motion appeared to strongly degrade the image quality, thereby influencing DKI parameters [12, 13]. We referred to past CT or MR images and first scanned the tumor with other sequences including T2- and fat-saturated T2-weighted sequences. If the tumor did not meet the above criteria, we canceled scanning of the DKI sequence.

The primary endpoint of this study was the comparison of MK between benign and malignant tumors. The secondary endpoint was to compare DKI parameters with minimum ADC (ADC_{min}) for differentiation between benign and malignant tumors. The mean MK (± SD) values of low-grade and high-grade gliomas were reported to be 0.484 ± 0.088 and 0.674 ± 0.113, with a difference of 0.19 in the mean MK [6]. To detect a difference of 0.19 in the degree of MK, ten patients each with a benign or malignant tumor were considered necessary with a power of 0.8 and two-sided p of 0.05 if the standard deviation (SD) was assumed to be 0.15 [16]. If the power was 0.9, 14 patients each were considered necessary. The difference in other tumors could be smaller, so we aimed to accrue at least 16 patients for both malignant and benign tumors. Patient accrual was continued until the patient number in both groups reached 16.

Between April 2016 and July 2017, a total of 47 patients (16 with malignant tumor) entered the study and underwent MR imaging with a DKI sequence on the 3-T MR scanner. Among these, one histologically diagnosed as myositis ossificans, one with uncertain diagnosis, one with old metastasis sustaining complete remission, and one with non-osteolytic bone tumor on CT were excluded from the study. Thus, 43 patients were accrued, comprising 25 men and 18 women. Their ages ranged from 18 to 90 years with a median age of 62 years. They were clinically or histologically confirmed as benign ($n = 27$) or malignant ($n = 16$). The 27 benign tumors were neurogenic tumors ($n = 21$), hemangioma ($n = 4$), suspected fibrous dysplasia ($n = 1$), and fibromyxoid tumor (n = 1). The fibromyxoid tumor and one neurogenic tumor were confirmed histologically, and the other 25 tumors were diagnosed clinically according to (1) the characteristic MR findings, (2) little or no changes for at least 1 year on follow-up imaging, and (3) clinical stability [3]. The 16 malignant tumors were bone osteolytic metastasis ($n = 5$), malignant myeloma ($n = 4$), soft tissue metastasis ($n = 2$), soft tissue sarcoma (n = 2), diffuse large B-cell lymphoma (n = 2), and malignant melanoma ($n = 1$). One malignant myeloma and one metastasis, two soft tissue sarcomas, two diffuse large B-cell lymphomas, and one malignant melanoma were confirmed histologically. The other nine tumors (three malignant myeloma and six metastasis) were diagnosed clinically based on (1) CT or MR findings, (2) increasing tumor size, and (3)

progression of the primary neoplasm or development of another metastasis. Their primary lesions were histologically confirmed except one that was clinically diagnosed as hepatocellular carcinoma by increasing AFP levels over 1000 ng/ml in addition to the imaging findings.

MR examination

All DKI images were obtained on the Hitachi 3-T MR scanner, using a two-dimensional (2D) diffusion-weighted spin-echo echoplanar imaging (SE-EPI) pulse sequence, four values of diffusion factor b (0, 1000, 1500, and 2000 s/mm^2), and 21 directions of diffusion gradients. We scanned the DKI sequence after routinely obtaining 2D T1-, T2-, and fat-saturated T2-weighted images. The imaging parameters for DKI were as follows: repetition time/echo time, 3000/84 ms; flip angle, 90°; number of excitations, 2 (b = 0, 1000 s/mm^2) and 4 (b = 1500, 2000 s/mm^2); field of view, 400 × 400 or 250 × 250 mm; matrix, 64 × 64 (with subsequent interpolation up to 128 × 128); slice thickness/gap, 5/1 mm; scanning plane, axial; parallel imaging factor, 2; and acquisition time, approximately 10 min.

Imaging analysis

A mean kurtosis (MK) map and conventional ADC map were calculated from the above-described DKI sequence on the MR console using a newly developed software program [14, 15]. The ADC map used for analysis was calculated from two values of diffusion factor (b = 0, 1000 s/mm^2) images. MR images were analyzed by two radiologists with 4 and 8 years of experience, respectively, in musculoskeletal tumor imaging. They were blinded to the clinical and pathological information. All images were presented in random order using PACS software (EV Insite R, PSP Corporation, Tokyo, Japan) and 3-megapixel monitors (Totoku, Tokyo, Japan) that allowed adjustment of the magnification, window, and level settings. The tumors were visually identified on diffusion-weighted images (b = 1000 s/mm^2), T2-weighted images, or other images. On the diffusion-weighted images (b = 1000 s/mm^2), elliptical regions of interest (ROIs) were manually selected within artifact-free and homogeneous high-intensity areas in the solid part of the tumors with enough distance from the edge but as large as possible. Care was taken to avoid cysts, necrosis, and fat. The selected ROIs were transferred to the MK and ADC map images, referring to previous studies [7, 10]. In the grayscale map, each pixel has values of MK and ADC, which are used for MK and ADC measurements on the ROIs. We used mean values of MK on the ROIs [6, 8–12]. Then, we calculated ADC_{min} values that were reported to be better correlated to tumor cellularity than the mean ADC values [2, 17]. In the above-mentioned ROIs, we placed three small ROIs presenting the lowest values on the ADC map. The lowest ADC value of the three small ROIs was used for ADC_{min} values according to previous studies [2, 17].

Statistical analysis

Statistical analysis was performed using BellCurve for Excel version 2.11 (Social Survey Research Information Co., Ltd., Tokyo, Japan). Mean values derived from the two observers' measurements were used for calculation, and interobserver agreement was evaluated using intra class correlation coefficient (ICC 2, 1). The Mann–Whitney *U* test was used to compare the MK and ADC_{min} values between benign and malignant tumors. Correlations between two values were analyzed by Spearman's rank correlation. Significance was set at $p < 0.05$. Receiver operating characteristic (ROC) analysis was carried out to determine suitable MK and ADC_{min} cutoff values for discrimination between benign and malignant tumors and to assess the diagnostic performance.

Results

Excellent interobserver agreement was obtained between the two observers regarding MK and ADC_{min} values: ICC = 0.98 and 0.99, respectively. MK values showed a strong correlation with ADC_{min} values (Fig. 1; Spearman's rs = 0.95; $p < 0.01$). Table 1 summarizes the histologic types of tumors (benign and malignant) and their MK and ADC_{min} values. The mean (± SD) MK values were 0.49 ± 0.17 and 1.14 ± 0.30 for benign and malignant tumors, respectively. The mean ADC_{min} values were $1.54 \pm 0.47 \times 10^{-3}$ mm^2/s and $0.60 \pm 0.16 \times 10^{-3}$ mm^2/s for benign and malignant tumors, respectively. Both MK and ADC_{min} values showed significant differences between benign and malignant tumors ($p < 0.01$). Table 2 presents the results of ROC analysis. At cutoffs of MK = 0.81, the specificity and sensitivity for the diagnosis of malignant tumors were 96.3 and 93.8%, respectively. At cutoffs of $ADC_{min} = 0.77 \times 10^{-3}$ mm^2/s, the specificity and sensitivity were 96.3 and 93.8%, respectively. The areas under the curve (AUC) were 0.97 and 0.99 for MK and ADC_{min}, respectively, with no difference ($p = 0.31$). Regarding the histologic types of tumors, the mean MK values were 0.98 ± 0.25 and 1.35 ± 0.30 for soft tissue or osteolytic metastasis ($n = 7$) and malignant myeloma ($n = 4$), respectively. The mean ADC_{min} values were $0.66 \pm 0.15 \times 10^{-3}$ mm^2/s and $0.59 \pm 0.17 \times 10^{-3}$ mm^2/s for metastasis and malignant myeloma, respectively. For differentiating metastasis and malignant myeloma, MK showed higher AUC than ADC_{min} values without significant difference (0.86 and 0.64, $p = 0.12$). For differentiating neurogenic tumor and hemangioma, there were no significant differences between the AUC values of MK and ADC_{min} (AUC = 0.64 and 0.54, $p = 0.28$). We did not perform ROC analysis for

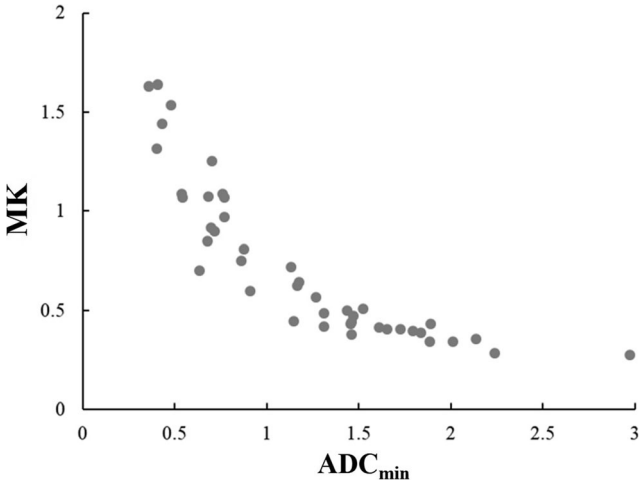

Fig. 1 Scatter plot of mean kurtosis (MK) and minimum apparent diffusion coefficient (ADC_{min}) values. MK values showed a strong correlation with ADC_{min} values (Spearman's rs = 0.95; $p < 0.01$)

other histologic tumor types due to the small number, $n = 1$ or 2.

Representative cases are presented in Figs. 2, 3, and 4, each showing the diffusion-weighted image (b = 1000 s/mm^2), MK map, and ADC map. Figure 2 shows a case of a benign tumor. Figures 3 and 4 show cases of malignant tumors.

Discussion

This study shows the utility of DKI and conventional ADC analysis to differentiate malignant and benign non-fatty musculoskeletal tumors. In malignant musculoskeletal tumors, MK showed significantly higher values and ADC_{min} showed significantly lower values than those in benign musculoskeletal tumors. DWI has emerged as a functional MRI technique without using contrast media, and increasing numbers of studies have been published on differentiation between malignant and benign lesions and diagnosis of various diseases in many parts of the human body [1–4, 6, 8–13, 18]. Conventional ADC analysis is based on Gaussian diffusion distribution. Thus, ADC values can be calculated by the difference in the signal intensity on diffusion-weighted images at multiple b values according to the monoexponential decay. Diffusion is random and isotropic in a perfectly homogenous medium [18]. However, water diffusion behavior in biological tissues is more complicated due to the complex cellular structures of tissues like membranes, so ADC values calculated by diffusion-weighted images using two low b values are actually different from those using two high b values.

Several advanced diffusion models have been proposed to account for the non-Gaussian diffusion behavior of biological tissues and to allow a more comprehensive analysis of diffusion-weighed images, such as intravoxel incoherent motion (IVIM), q-space imaging, and DKI. IVIM considers a biexponential model, separately evaluating the microcirculation of blood within the capillaries (perfusion) and pure molecular diffusion. However, the true behavior of molecular diffusion is more complicated due to adjacent cell membranes and other microstructures, so this biexponential model may not be reliable for explaining diffusion behaviors in complex biological tissues [8, 9, 19]. The most comprehensive and rigorous method proposed is the q-space imaging, which employs a multi-exponential model. This method measures diffusion-weighted signals with many different gradient strengths and diffusion times and provides a direct measure of water diffusion restriction in the tissue. However, the disadvantage of sampling using the complete q-space method is the extraordinarily long scan time and b values as high as 30,000 s/mm^2, which are currently impractical on clinically used scanners [19].

DKI represents the deviation of tissue diffusion from a Gaussian model, which is thought to be correlated with the complexity of tumor microenvironment. This sequence is

Table 1 Summary of the histologic types of musculoskeletal tumors (benign and malignant) and values of MK and ADC_{min}

Lesions	Number	Mean MK	Mean ADC_{min} ($\times 10^{-3}$ mm^2/s)
Benign lesion (total)	27	0.49 ± 0.17	1.54 ± 0.47
Neurogenic tumor	21	0.49 ± 0.17	1.49 ± 0.38
Hemangioma	4	0.54 ± 0.20	1.63 ± 0.94
Fibrous dysplasia	1	0.34	1.89
Fibromyxoid lesion	1	0.39	1.84
Malignant lesions (total)	16	1.14 ± 0.30	0.60 ± 0.16
Bone osteolytic metastasis	5	0.94 ± 0.29	0.67 ± 0.16
Malignant myeloma	4	1.35 ± 0.30	0.59 ± 0.17
Soft tissue metastasis	2	1.08 ± 0.01	0.65 ± 0.16
Soft tissue sarcoma	2	1.00 ± 0.11	0.69 ± 0.10
Diffuse large B-cell lymphoma	2	1.35 ± 0.40	0.45 ± 0.13
Malignant melanoma	1	1.32	0.40

Values are mean ± SD. *MK* mean kurtosis, *ADC_{min}* minimum apparent diffusion coefficient

Table 2 Receiver operating characteristic analysis for MK and ADC_{min} in the differentiation between benign and malignant musculoskeletal tumors

Parameters	AUC	Cutoff value	Specificity	Sensitivity	*p* value
MK	0.97	0.81	96.3%	93.8%	< 0.01
ADC_{min}	0.99	0.77 ($\times 10^{-3}$ mm^2/s)	96.3%	93.8%	< 0.01

MK mean kurtosis, ADC_{min} minimum apparent diffusion coefficient, *AUC* area under the curve

clinically feasible; the calculation by diffusion-weighted images with three or more b values allows a relatively short scan time, using moderately high b values (up to around 2500 s/mm^2) that can be practically used in a clinical situation [6–11, 19, 20]. Thus, the use of DKI has been extended from brain tumors to head and neck, rectal, prostate, and breast tumors as mentioned in the Introduction section. However, there have been few DKI studies of musculoskeletal tumors. One of the reasons for this is thought to be that the DKI parameter is sensitive to noise effects or degradation of image quality, which are a strong influence in non-brain imaging. Musculoskeletal tumors can occur in any part of the body, and the associated image noise and artifacts of diffusion-weighted images are varied, being influenced by the body part, shape of the subject, receiver coil, and susceptibility artifacts caused by air or bone. Furthermore, most previous studies of DKI have used diverse methods of analysis and calculation chosen by the user, so reliability has not been confirmed. For a more reliable calculation in musculoskeletal tumors, we used the recently developed commercial DKI analysis software, which optimizes the scan parameters and algorithm [14, 15]. This software includes a spatial smoothing filter to reduce noise effects. Additionally, we employed a 3-T MR scanner to benefit from its lower noise effect compared with a 1.5-T scanner. The MK values showed a strong correlation with ADC_{min} values in our study, as previously reported for other tumors [6–10], which suggested that we obtained reliable DKI calculations.

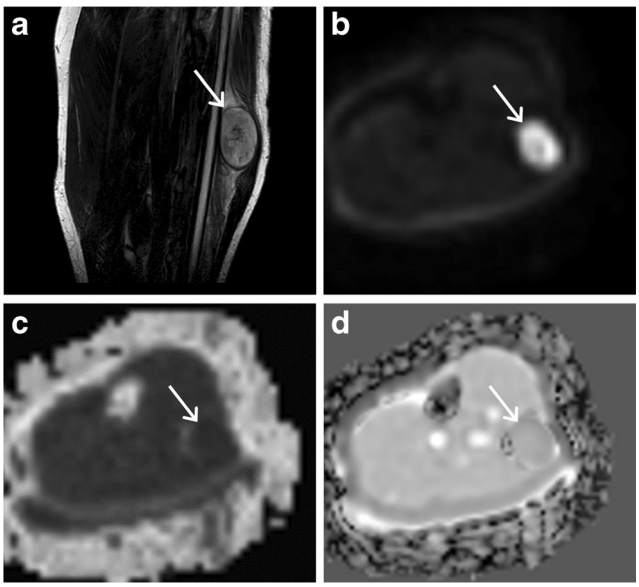

Fig. 2 A 60-year-old woman clinically diagnosed with neurogenic tumor. The tumor is indicated by the *arrows* on coronal T2-weighted image (**a**), axial diffusion-weighted image (b = 1000 s/mm^2) (**b**), MK map (**c**), and ADC map (**d**). The MK and ADC_{min} values of the tumor were 0.45 and 1.15×10^{-3} mm^2/s, respectively

Previous studies reported that DKI parameters were more strongly correlated with the brain glioma grade [6, 7], and DKI showed higher diagnostic performance in differentiating malignant and benign tumors in previous prostate and breast studies [9, 10]. In this study, both the MK and ADC_{min} values showed high diagnostic performance in differentiating benign and malignant tumors with high AUC scores. The required sample size was calculated with the aim of comparing MK values between benign and malignant tumors, and we found that the MK values of malignant tumors were quite different from those of benign tumors (1.14 ± 0.30 and 0.49 ± 0.17, respectively) with that sample size. Nevertheless, both MK and ADC_{min} showed very high scores of AUC (0.97 and 0.99, respectively), so the superiority of DKI over ADC_{min} was not confirmed. In malignant tumors, DKI showed higher AUC than ADC_{min} values in differentiating metastasis and malignant myeloma, but there was no significant difference (0.86 and 0.64, $p = 0.12$) and the sample sizes were insufficient ($n = 7$ and 4, respectively). Also, our study included no cases of myxoid sarcoma or chondrosarcoma, which would show significant overlaps of ADC_{min} values compared to benign tumors [21, 22]. Myxoid sarcoma and chondrosarcoma might show significantly higher MK values than benign tumors, because tumor microenvironment in sarcoma is considered to be more complex than in benign tumors. DKI might improve differentiation between benign and malignant tumors with a myxoid or chondroid component. Furthermore, the utility of ADC_{min} for monitoring the chemotherapeutic response of osteosarcoma was reported [17], so DKI may also be useful for monitoring the therapeutic response of malignant musculoskeletal tumors. Analysis with a higher number of subjects will be necessary to differentiate various histologic types of musculoskeletal tumors or assess therapeutic response of malignant musculoskeletal tumors. Additionally, combined analysis using DKI and ADC_{min} may contribute to a more accurate evaluation. Further studies are warranted.

In this study, the acquisition time was approximately 10 min using 21 diffusion directions. The reliabilities of axial kurtosis and radial kurtosis were insufficient when the number of diffusion directions was less than 20 [14]. Diffusion tensor imaging (DTI), one of the Gaussian DWI techniques, can

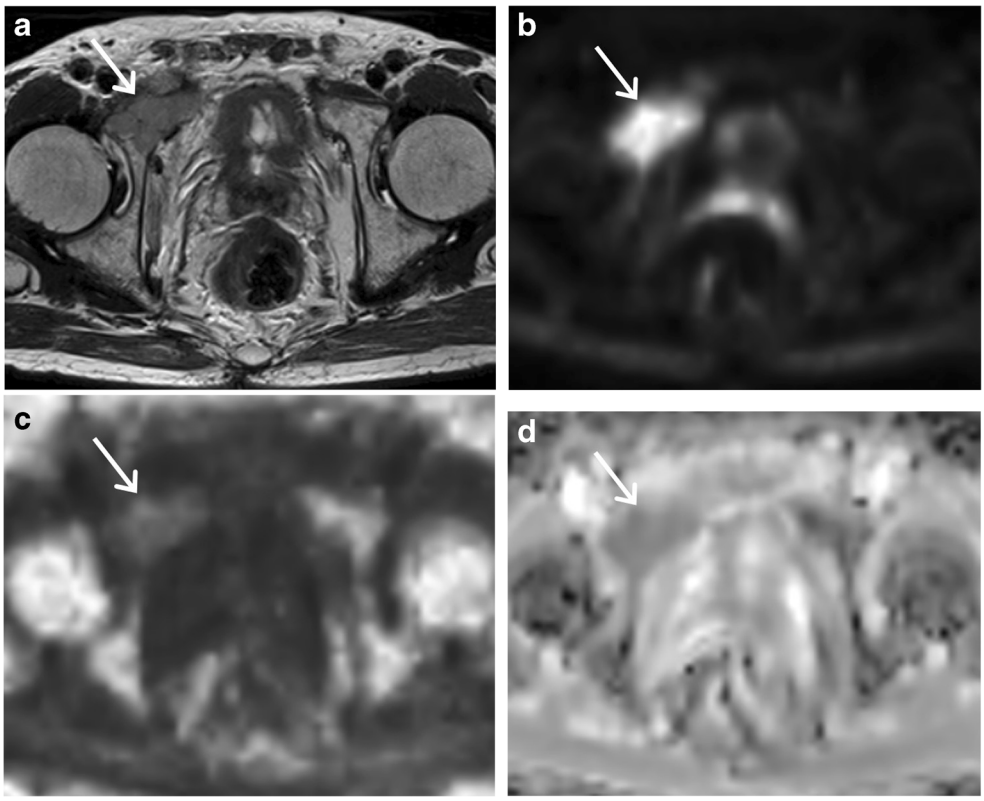

Fig. 3 A 63-year-old man clinically diagnosed with osteolytic bone metastasis. A metastatic tumor in the pubic bone is indicated by the *arrow* on axial T2-weighted image (**a**), axial diffusion-weighted image ($b = 1000$ s/mm^2) (**b**), MK map (**c**), and ADC map (**d**). The MK and ADC_{min} values of the tumor were 0.88 and 0.72×10^{-3} mm^2/s, respectively

detect and quantify the anisotropy of diffusion by using a high number of diffusion directions [18]. Water diffusion in the brain white matter is anisotropic and is influenced by fiber orientation. DTI provides micro-architectural details of white matter tracts such as the pyramidal tract for intraoperative navigation purposes. Also, DKI can calculate the anisotropy of diffusion kurtosis by using a high number of diffusion directions. A previous study reported that decreased axial

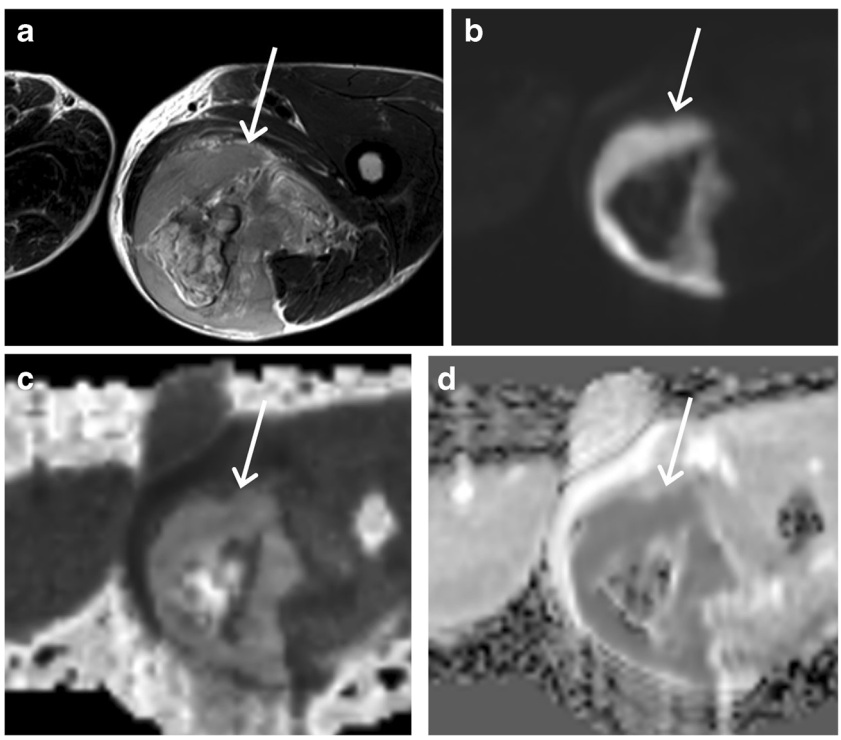

Fig. 4 A 71-year-old man histologically diagnosed with diffuse large B-cell lymphoma. The *arrows* indicate the tumor on axial T2-weighted image (**a**), axial diffusion-weighted image ($b = 1000$ s/mm^2) (**b**), MK map (**c**), and ADC map (**d**). The MK and ADC_{min} values of the tumor were 1.07 and 0.54×10^{-3} mm^2/s, respectively

kurtosis in DKI and increased radial diffusivity in DTI are sensitive to schizophrenia and may suggest axonal damage and myelin impairment [20]. However, we should not consider a single fiber orientation in tumor environment, in contrast to the brain white matter tract. A previous DKI report on brain glioma grade showed that DTI was not helpful in evaluating either glioma grade or cellular proliferation [6]. We thus did not use axial or radial kurtosis or DTI. We only used MK, the average kurtosis of all diffusion directions, which we could calculate with a relatively small number of diffusion directions. A previous DKI study evaluating the spinal cord used six diffusion directions and argued that six directions were sufficient for calculating MK [12]. Therefore, although we used 21 diffusion directions, the scan time may be reduced to one-third with a small increase in image noise if we use seven diffusion directions.

Our study has several limitations. First, the ROIs in the tumors were manually selected. Thus, the MK and ADC_{min} values may be different depending on the determined ROIs when the distributions of MK and ADC value were inhomogeneous in a tumor. Nevertheless, excellent interobserver agreement was obtained and the reliability was confirmed. Second, we did not include small tumors (< 2 cm) and tumors in the chest, hand, or foot. This is because susceptibility artifacts caused by air or distortion, motion artifacts from breathing, and partial volume effects might strongly influence the reliability of the MK value. Nevertheless, accurate calculation of the MK value may be possible for lower signal-to-noise ratio images. Further DKI studies on reliability in the chest, hand, and foot are warranted. Third, we included both soft tissue and osteolytic bone tumors. Benign osteolytic and malignant soft tissue tumors are much fewer than malignant bone and benign soft tissue tumors, so accumulating enough numbers of samples was difficult if we limited the study to either soft tissue or bone tumors. We included osteolytic lesions completely showing soft tissue density without calcification on CT images, but fundamental differences between bone and soft tissue tumors may influence diffusion properties. For evaluating DKI and other diffusion parameters, either soft tissue or bone tumors should be included. Fourth, histological confirmation was not available for many tumors. Nevertheless, most benign tumors were diagnosed by the characteristic MR findings and followed for at least 1 year. For nine malignant tumors not histologically confirmed, their primary lesions were histologically confirmed in eight and one hepatocellular carcinoma was diagnosed by typical imaging findings and high AFP levels (> 1000 ng/ml).

In conclusion, DKI showed high diagnostic accuracy in differentiating malignant and benign musculoskeletal tumors, similar to conventional ADC analysis. While there have been no previous DKI studies on musculoskeletal tumors, we confirmed reliability of DKI calculation. However, no clear added value of DKI could be demonstrated in differentiating musculoskeletal tumors. Further studies on DKI analysis to differentiate specific musculoskeletal tumor types or assess therapeutic response of malignant musculoskeletal tumors and combined analysis of DKI and ADC are warranted.

Compliance with ethical standards

Conflict of interest There are no financial or other conflicts of interest in relation to this paper.

References

1. Surov A, Nagata S, Razek AA, Tirumani SH, Wienke A, Kahn T. Comparison of ADC values in different malignancies of the skeletal musculature: a multicentric analysis. Skelet Radiol. 2015;44(7):995–1000.
2. Teixeira PA, Gay F, Chen B, Zins M, Sirveaux F, Felblinger J, et al. Diffusion-weighted magnetic resonance imaging for the initial characterization of non-fatty soft tissue tumors: correlation between T2 signal intensity and ADC values. Skelet Radiol. 2016;45(2):263–71.
3. Ahlawat S, Khandheria P, Subhawong TK, Fayad LM. Differentiation of benign and malignant skeletal lesions with quantitative diffusion weighted MRI at 3T. Eur J Radiol. 2015;84(6):1091–7.
4. Surov A, Behrmann C. Diffusion-weighted imaging of skeletal muscle lymphoma. Skelet Radiol. 2014;43(7):899–903.
5. Karchevsky M, Babb JS, Schweitzer ME. Can diffusion-weighted imaging be used to differentiate benign from pathologic fractures? A meta-analysis. Skelet Radiol. 2008;37(9):791–5.
6. Jiang R, Jiang J, Zhao L, Zhang J, Zhang S, Yao Y, et al. Diffusion kurtosis imaging can efficiently assess the glioma grade and cellular proliferation. Oncotarget. 2015;6(39):42380–93.
7. Tonoyan AS, Pronin IN, Pitshelauri DI, Shishkina LV, Fadeeva LM, Pogosbekyan EL, et al. A correlation between diffusion kurtosis imaging and the proliferative activity of brain glioma. Zh Vopr Neirokhir Im N N Burdenko. 2015;79(6):5–14.
8. Yuan J, Yeung DK, Mok GS, Bhatia KS, Wang YX, Ahuja AT, et al. Non-Gaussian analysis of diffusion weighted imaging in head and neck at 3T: a pilot study in patients with nasopharyngeal carcinoma. PLoS One. 2014;9(1):e87024.
9. Tamura C, Shinmoto H, Soga S, Okamura T, Sato H, Okuaki T, et al. Diffusion kurtosis imaging study of prostate cancer: preliminary findings. J Magn Reson Imaging. 2014;40(3):723–9.
10. Wu D, Li G, Zhang J, Chang S, Hu J, Dai Y. Characterization of breast tumors using diffusion kurtosis imaging (DKI). PLoS One. 2014;9(11):e113240.
11. Hu F, Tang W, Sun Y, Wan D, Cai S, Zhang Z, et al. The value of diffusion kurtosis imaging in assessing pathological complete response to neoadjuvant chemoradiation therapy in rectal cancer: a comparison with conventional diffusion-weighted imaging. Oncotarget. 2017.
12. Hori M, Tsutsumi S, Yasumoto Y, Ito M, Suzuki M, Tanaka FS, et al. Cervical spondylosis: evaluation of microstructural changes in spinal cord white matter and gray matter by diffusional kurtosis imaging. Magn Reson Imaging. 2014;32(5):428–32.
13. Glenn GR, Tabesh A, Jensen JH. A simple noise correction scheme for diffusional kurtosis imaging. Magn Reson Imaging. 2015;33(1):124–33.
14. Yokosawa S, Sasaki M, Bito Y, Ito K, Yamashita F, Goodwin J, et al. Optimization of scan parameters to reduce acquisition time for

diffusion kurtosis imaging at 1.5T. Magn Reson Med Sci. 2016;15(1):41–8.
15. Yokosawa S, Ochi S, Bito Y, Ito K, Sasaki M. Robust estimation with suppressed image blurring for diffusion kurtosis imaging using selective spatial smoothing filter. Proc Intl Soc Magn Reson Med. 2014;2581.
16. Motulsky H. Appropriate simple size. In: Motulsky H, editor. Trans intuitive biostatics. Tokyo: Science Medical; 1997. p. 196–205.
17. Oka K, Yakushiji T, Sato H, Hirai T, Yamashita Y, Mizuta H. The value of diffusion-weighted imaging for monitoring the chemotherapeutic response of osteosarcoma: a comparison between average apparent diffusion coefficient and minimum apparent diffusion coefficient. Skelet Radiol. 2010;39(2):141–6.
18. Baliyan V, Das CJ, Sharma R, Gupta AK. Diffusion-weighted imaging: technique and applications. World J Radiol. 2016;8(9):785–98.
19. Zhuo J, Xu S, Proctor JL, Mullins RJ, Simon JZ, Fiskum G, et al. Diffusion kurtosis as an in vivo imaging marker for reactive astrogliosis in traumatic brain injury. NeuroImage. 2012;59(1):467–77.
20. Zhu J, Zhuo C, Qin W, Wang D, Ma X, Zhou Y, et al. Performances of diffusion kurtosis imaging and diffusion tensor imaging in detecting white matter abnormality in schizophrenia. Neuroimage Clin. 2015;7:170–6.
21. Nagata S, Nishimura H, Uchida M, Sakoda J, Tonan T, Hiraoka K, et al. Diffusion-weighted imaging of soft tissue tumors: usefulness of the apparent diffusion coefficient for differential diagnosis. Radiat Med. 2008;26(5):287–95.
22. Douis H, Jeys L, Grimer R, Vaiyapuri S, Davies AM. Is there a role for diffusion-weighted MRI (DWI) in the diagnosis of central cartilage tumors? Skelet Radiol. 2015;44(7):963–9.